



# Salt-template synthesis of mesoporous carbon monolith for ionogel-based supercapacitors

Shan Zhu, Pierre-Louis Taberna, Naiqin Zhao, Patrice Simon

## ► To cite this version:

Shan Zhu, Pierre-Louis Taberna, Naiqin Zhao, Patrice Simon. Salt-template synthesis of mesoporous carbon monolith for ionogel-based supercapacitors. *Electrochemistry Communications*, 2018, 96, pp.6-10. 10.1016/j.elecom.2018.09.003 . hal-02048309

**HAL Id: hal-02048309**

**<https://hal.science/hal-02048309>**

Submitted on 25 Feb 2019

**HAL** is a multi-disciplinary open access archive for the deposit and dissemination of scientific research documents, whether they are published or not. The documents may come from teaching and research institutions in France or abroad, or from public or private research centers.

L'archive ouverte pluridisciplinaire **HAL**, est destinée au dépôt et à la diffusion de documents scientifiques de niveau recherche, publiés ou non, émanant des établissements d'enseignement et de recherche français ou étrangers, des laboratoires publics ou privés.






## Open Archive Toulouse Archive Ouverte (OATAO)

OATAO is an open access repository that collects the work of Toulouse researchers and makes it freely available over the web where possible

This is an author's version published in: <http://oatao.univ-toulouse.fr/21789>

**Official URL:** <https://doi.org/10.1016/j.elecom.2018.09.003>

### To cite this version:

Zhu, Shan  and Taberna, Pierre-Louis  and Zhao, Naiqin and Simon, Patrice  *Salt-template synthesis of mesoporous carbon monolith for ionogel-based supercapacitors.* (2018) *Electrochemistry Communications*, 96. 6-10. ISSN 1388-2481

Any correspondence concerning this service should be sent  
to the repository administrator: [tech-oatao@listes-diff.inp-toulouse.fr](mailto:tech-oatao@listes-diff.inp-toulouse.fr)

# Salt-template synthesis of mesoporous carbon monolith for ionogel-based supercapacitors

Shan Zhu<sup>a,b,c</sup>, Pierre-Louis Taberna<sup>a,b</sup>, Naiqin Zhao<sup>c,\*</sup>, Patrice Simon<sup>a,b,\*\*</sup>

<sup>a</sup> CIRIMAT UMR CNRS 5085 Université Paul Sabatier Toulouse III, 118 route de Narbonne, 31062 Toulouse, France

<sup>b</sup> Réseau sur le Stockage Electrochimique de l'Energie (RS2E), FR CNRS 3459, France

<sup>c</sup> School of Materials Science and Engineering and Tianjin Key Laboratory of Composites and Functional Materials, Tianjin University, Tianjin 300350, China

## ARTICLE INFO

### Keywords:

Carbon monolith

Mesopores

Salt template

Ionogel

Solid-state supercapacitors

## ABSTRACT

Mesoporous carbon monoliths (MCM) were prepared by using soluble salt as templates. During the synthesis, a freeze-drying process enables a surface coating of self-assembled Na<sub>2</sub>SiO<sub>3</sub> salt particles with sucrose, which is further transformed into carbon by heat treatment. After removal of the salt templates by washing, MCM were obtained. MCM samples exhibit high specific surface area together with high mesoporous volume, whose pore sizes can be tuned from 10 to 30 nm by adjusting the ratio between salt and carbon sources. MCM materials were further used as electrodes in combination with ionogel electrolyte to assemble a solid-state supercapacitor. In this configuration, MCM electrodes show capacitance as high as 75 F g<sup>-1</sup> and good rate performance thanks to the carbon monolith pore size selected.

## 1. Introduction

Supercapacitors are electrochemical energy storage devices suited for high power delivery and energy harvesting applications [1]. According to Eq. (1),

$$E = \frac{CV^2}{7.2} \quad (1)$$

The energy density  $E$  (Wh/kg) is proportional to the specific capacitance  $C$  (F g<sup>-1</sup>) and the square of voltage window  $V$  (V). Careful selection of electrolytes with large voltage window is then an efficient way to achieve high energy density [2]. Currently, aqueous electrolytes such as KOH or H<sub>2</sub>SO<sub>4</sub> are limited by narrow potential window (< 2 V), because of water decomposition. Therefore, nonaqueous electrolytes including organic electrolytes and ionic liquids have attracted great attention [3–5]. Conventional acetonitrile- or propylene-based organic electrolytes used in commercial cells can achieve voltage windows up to 2.85 V [6]; however, they are usually flammable and toxic, which makes electrolyte leaks and packaging key issues to solve. Flammability issue can be in part addressed using solvent-free ionic liquids electrolyte, which can achieve voltage window as high as 3.5 V thanks to their low vapor pressure and thermal stability [3–6]. However, the low ionic conductivity limits their use as electrolytes in conventional supercapacitor cells. Electrolyte leak is not only a serious issue for

supercapacitor but also for micro-supercapacitors; this explains why a lot of solid-state like electrolytes have been recently developed, to be used in combination with porous carbon electrodes [7]. Most of these solid-state like electrolytes are based on gels or polymers swelled with aqueous-based or water-containing electrolytes, leading to voltage window below 2 V.

Ionogels, which are ionic liquids entrapped into a SiO<sub>2</sub> matrix, have been recently proposed as solid-state electrolyte for supercapacitors [5]. Due to the solid-state features, ionogel not only makes high operating voltage possible, but also solved the abovementioned problems of liquid-type electrolyte [3–5]. Maboudian et al. used ionogel in a micro-supercapacitor device and achieved the energy density of 3 mWh cm<sup>-3</sup> [7]. Our group assembled a solid-state supercapacitor using ionogel electrolyte, which can be operated in a large temperature range and led to the capacitance of 150 mF cm<sup>2</sup> [4,5]. However, all of the reported ionogel electrolyte-based devices used microporous carbon (e.g. activated carbon) as electrodes due to their high specific surface area (SSA). The effects of pore size distribution have not yet been specifically studied. Also, all studies dedicated to ionogel as supercapacitor electrolytes used porous carbon powders coated onto supporting current collectors, which makes the assembly of solid-state like full cells complicated.

Carbon monoliths are a kind of self-supported three-dimensional carbon structure. They combine advantages of high electrical

\* Corresponding author.

\*\* Correspondence to: CIRIMAT UMR CNRS 5085 Université Paul Sabatier Toulouse III, 118 route de Narbonne, 31062 Toulouse, France.

E-mail addresses: [nqzhao@tju.edu.cn](mailto:nqzhao@tju.edu.cn) (N. Zhao), [simon@chimie.ups-tlse.fr](mailto:simon@chimie.ups-tlse.fr) (P. Simon).

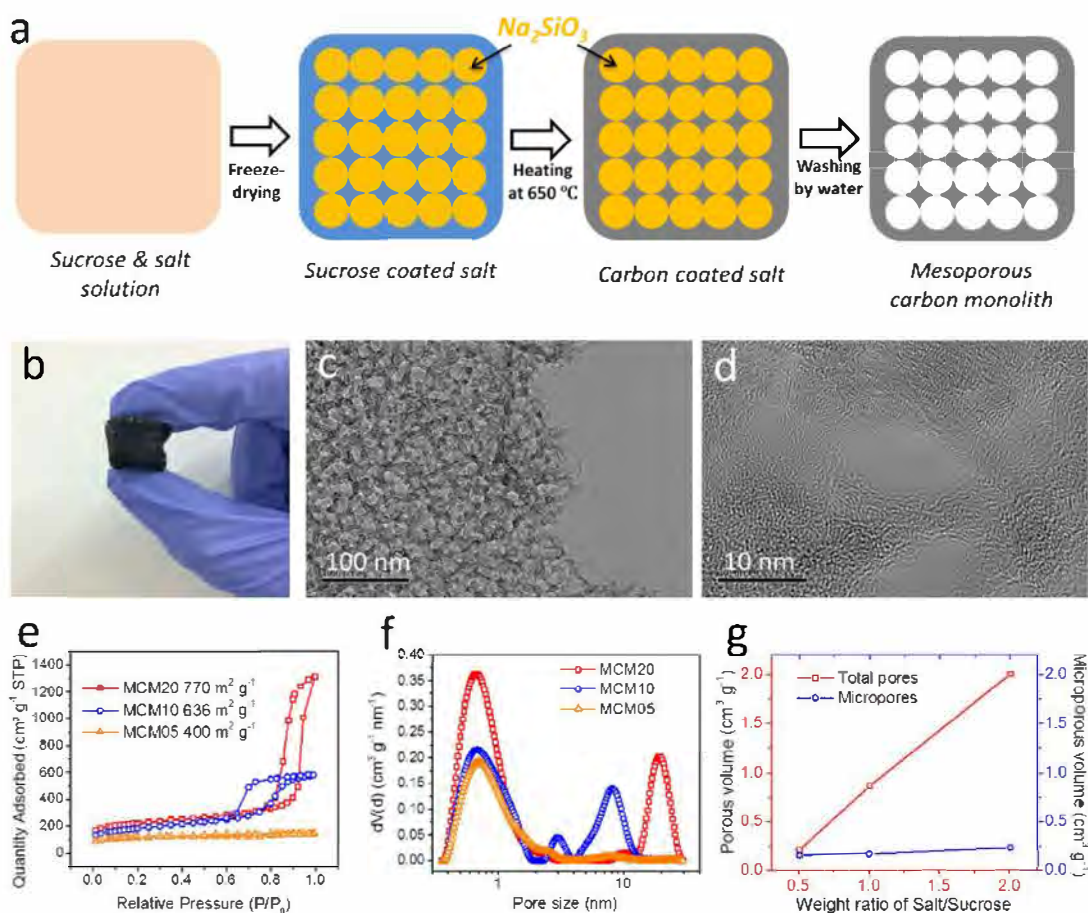


**Fig. 1.** (a) Illustration of MCM preparation process. (b) Picture and (c,d) TEM images of MCM20. (e) Nitrogen isothermal adsorption/desorption curves (quantity of  $\text{N}_2$  gas adsorbed is the equivalent volume recalculated in STP) and (f) pore size distribution (Y-axis is the porous volume) of MCM samples. (g) The relation of salt/sucrose ratio and the pores volumes.

conductivity ( $10^3$ – $10^6 \text{ S cm}^{-1}$ ) [8,9], easy shaping ability and mechanical stability [10]. Compared with porous carbon powder, self-supported carbon monoliths can be directly used as electrode without adding electrochemically inactive binders or conducting additives. Also, 3D monolith carbon structures with interconnected pores enhance mass-transfer kinetics. Finally, carbon monoliths must achieve high SSA for increasing charge storage, and abundant pore interconnections for enhancing electrolyte accessibility [8–10], which is even more important for ionogel.

In this paper, we report a facile and scalable approach to synthesize mesoporous carbon monolith (MCM) by using soluble salt template methods, for a final use as supercapacitor electrode in combination with solid-state like ionogel electrolyte. The synthesis method allows tuning of the carbon monolith pore size distribution while maintaining SSA as high as possible ( $> 600 \text{ m}^2 \text{g}^{-1}$ ), by adjusting the ratio of carbon source and salt. As-prepared MCM were selected to operate in ionogel electrolyte for a high performance solid-state supercapacitor.

## 2. Experimental

### 2.1. Synthesis of MCM

1.0 g carbon precursor (sucrose) and 0.5–2.0 g salt template (sodium metasilicate nonahydrate,  $\text{Na}_2\text{SiO}_3 \cdot 9\text{H}_2\text{O}$ ) were dissolved in 20 mL deionized water. The solution was frozen in nitrogen liquid and moved to a lyophilizer (Alpha 1-4 LDplus, CHRIST). After for 3 days freeze-drying process at  $-80^\circ\text{C}$  in vacuum, a mixture of salt and sucrose monolith was obtained. The monolith was further heated to  $650^\circ\text{C}$  for 2 h with the heating rate of  $5^\circ\text{C}/\text{min}$  under 1:1  $\text{Ar}/\text{H}_2$  atmosphere. The

salt template was washed out using water, and a second freeze-drying process was achieved to remove the residual water before the final MCM were obtained. The obtained samples were named as MCM05, MCM10 and MCM20 according to the initial salt content (0.5, 1.0 and 2.0 g).

### 2.2. Synthesis of ionogel

The ionogel was prepared by a sol-gel process [4,5]: 0.35 mL tetramethyl orthosilicate, 0.25 mL tetraethyl orthosilicate, and 1.0 mL ionic liquid 1-ethyl-3-methylimidazolium bis(trifluoromethylsulfonyl) imide [EMITFSI] were mixed together to obtain a transparent solution. Then, 0.5 mL isopropanol, 0.2 mL deionized water and 0.1 mL hydrochloric acid (37%) were added into the mixture solution. The obtained mixture was kept at  $60^\circ\text{C}$  for 10 min under stirring (300 rpm). After that, the resulting solution was casted in sealed cylindrical containers and kept for 24 h at room temperature for gelation and then dried at  $80^\circ\text{C}$  for one week. At the end, a self-standing ionogel without any liquid leakage was obtained.

### 2.3. Characterization and electrochemical tests

Transmission electron microscopy (TEM) images were obtained on a FEI Tecnai G2 F20 TEM (Japan). Nitrogen sorption isotherm was carried out on ASAP 2020 Plus Physisorption (USA). MCM were cut into target shapes and were used as electrodes directly without any binders. 2- and 3-electrode Swagelok cells were used to run electrochemical characterizations. 3-electrode tests were carried out using one piece of MCM film ( $5.0 \text{ mg cm}^{-2}$ ) as working electrode, a YP50 (Kuraray

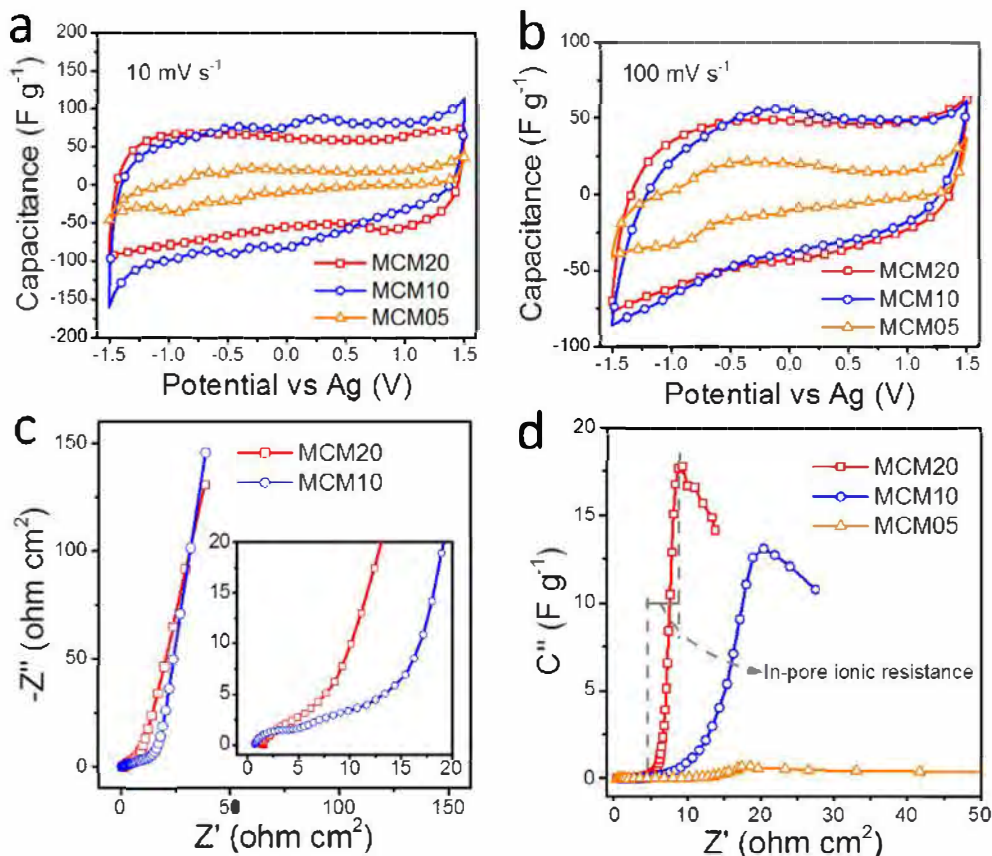


**Fig. 2.** Electrochemical characterizations of MCM in EMITFSI electrolyte: CV curves at (a)  $10 \text{ mV s}^{-1}$  and (b)  $100 \text{ mV s}^{-1}$ . (c) Nyquist plots of MCM20 and MCM10. (d) Imaginary capacitance ( $C''$ ) v.s. real impedance ( $Z'$ ) plot of MCM.

company) porous carbon film as counter electrode ( $> 50 \text{ mg cm}^{-2}$ ) and an Ag rod as reference electrode. Platinum discs were used as current collectors. In 2-electrode set-up, two pieces of MCM film with the same weight were used as electrodes. Electrochemical impedance spectroscopy (EIS) measurements were carried out at open circuit voltage (OCP) with an amplitude of  $\pm 10 \text{ mV}$  within a frequency range from  $200 \text{ kHz}$  to  $0.01 \text{ Hz}$ . Capacitance was calculated from cyclic voltammogram (CV) by measuring the slope of the charge calculated during cathodic sweep plotted versus cell voltage. Capacitance of MCM samples in solid-state supercapacitor devices were obtained by dividing twice the cell capacitance by the MCM weight per electrode. All Swagelok cells were tested at room temperature by using a VMP3 potentiostat (Biologic, France).

### 3. Results and discussion

Fig. 1a shows a sketch of the salt-template synthesis method. A solution of carbon precursor (sucrose) and soluble salt ( $\text{Na}_2\text{SiO}_3$ ) was freeze-dried, to promote the self-assembly of crystallized salt coated with sucrose to form the templates [11]. Sucrose was then carbonized into carbon by heat treatment under inert atmosphere. After further washing of the carbon/salt monolith with deionized water to remove salt, MCM were obtained (Fig. 1a). As shown in the Fig. 1b, self-supported bulk carbon was obtained, suggesting high mechanical stability. TEM observations of MCM20 revealed its 3D interconnected mesoporous network, with pore sizes around  $20 \text{ nm}$  (Fig. 1c,d).

$\text{N}_2$  gas sorption measurements were conducted to further study the microstructures of MCM (Fig. 1e). SSAs of samples were found to increase with increasing content of salt, from  $400 \text{ m}^2 \text{ g}^{-1}$  of MCM05 to  $770 \text{ m}^2 \text{ g}^{-1}$  of MCM20. Also, both of MCM20 and MCM10 show a type IV isotherm with hysteresis loops at a relative pressure in the range of

$0.60\text{--}0.97$ , indicating the existence of mesopores [12]. As shown in the pore size distribution (Fig. 1f), porous structure of MCM contains mesopores and micropores. According to previous reports, micropores stem from the carbonization of sucrose while mesopores are derived from the salt template [11]. Moreover, increasing the amount of  $\text{Na}_2\text{SiO}_3$  results in the change of the mesopore size distribution: from no obvious mesopores (MCM05), to  $5\text{--}12 \text{ nm}$  pores with an average mesoporous pore size of  $7 \text{ nm}$  (MCM10) and finally to  $15\text{--}30 \text{ nm}$  with an average pore size of  $18 \text{ nm}$  (MCM20). MCM20 exhibits the highest porous volume ( $2.0 \text{ cm}^3 \text{ g}^{-1}$ ), and  $88\%$  of which comes from mesopores (Fig. 1g). By comparison, mesoporous volume of MCM10 accounts for  $80\%$  of the total pore volume ( $0.86 \text{ cm}^3 \text{ g}^{-1}$ ). Thus, increasing the salt over carbon source ratio enables the control of the mesoporous structure of MCM, giving opportunity to provide electrolyte reservoir [12]. If the weight ratio of salt/sucrose is larger than 2, no self-standing monolith is achievable.

The capacitive properties of MCM were investigated in 3-electrode set-up configuration. In neat EMITFSI electrolyte, CV curves of MCM20 and MCM10 recorded at  $10 \text{ mV s}^{-1}$  show a capacitive behavior with rectangular-like shape; capacitance of respectively  $65$  and  $70 \text{ F g}^{-1}$  could be achieved, respectively for MCM20 and MCM10 (Fig. 2a) within  $3 \text{ V}$  voltage window [13]. Up to  $100 \text{ mV s}^{-1}$ , MCM20 and MCM10 still keep their double-layer charge storage features (Fig. 2b). In contrast, the MCM05 sample showed poor electrochemical behavior at both  $10$  and  $100 \text{ mV s}^{-1}$ , as it was expected from low specific surface area and low mean pore size ( $< 0.6 \text{ nm}$ ) [14,15].

Fig. 2c shows the Nyquist plots of the two samples recorded at OCP. Both samples exhibit similar high frequency resistance ( $< 2 \Omega \text{ cm}^2$ ), since these resistances are constituted of the ionic resistance of the electrolyte and the intrinsic resistance of the electrode [16]. In the middle frequency range, the low-frequency capacitive behavior of



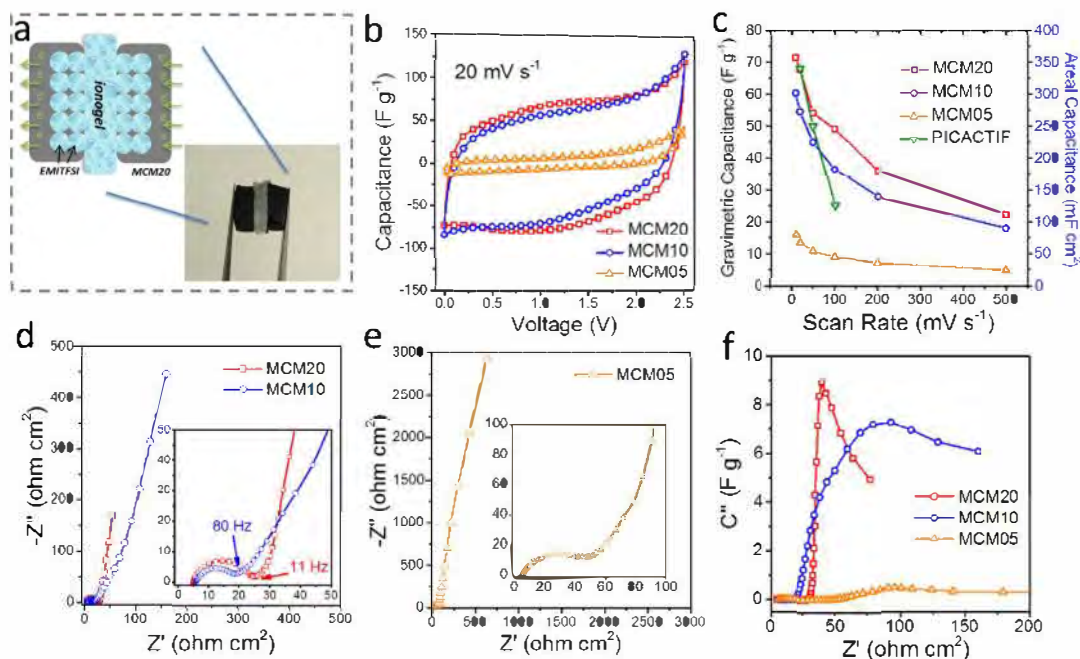


**Fig. 3.** (a) Sketch and image of a MCM-ionogel-MCM solid-state supercapacitor. Performance of ionogel-based supercapacitors: (b) CV curves at  $20 \text{ mV s}^{-1}$  and (c) specific capacitances per electrode at various scan rates of MCM and PICACTIF carbon (reproduced from Ref. [5]). (d) Nyquist plots for MCM20, MCM10 and (e) MCM05 electrode. (f) Imaginary capacitance ( $C''$ ) v.s. real impedance ( $Z'$ ) plot of MCM samples.

MCM10 is shifted along the real axis toward more resistive values. Also, MCM20 exhibits a faster capacitive signature as can be seen from the sharp increase of the imaginary part of the capacitance [17], associating with the presence of larger mesopores in MCM20. In Fig. 2d, the in-pore ionic resistances were calculated to be  $4$ ,  $14$  and  $12 \Omega \text{ cm}^2$  for MCM20, MCM10, and MCM05 respectively. These values suggest that ions transfer more efficiently in the pore channels of MCM20.

As illustrated in Fig. 3a, a solid-state like supercapacitor was assembled by combining MCM together with ionogel. Fig. 3b shows the CV curves between  $0 \text{ V}$  and  $2.5 \text{ V}$  of MCM-ionogel supercapacitor at  $20 \text{ mV s}^{-1}$ . The rectangular-shape of CVs confirmed the capacitive electrochemical signatures of MCM. Consequently, the specific capacitance of MCM20 electrode was up to  $75 \text{ F g}^{-1}$  ( $375 \text{ mF cm}^{-2}$ ) at  $10 \text{ mV s}^{-1}$  per electrode, which is higher than the value of MCM10 ( $62 \text{ F g}^{-1}$ ) and MCM05 ( $17 \text{ F g}^{-1}$ ). MCM20 retained its surpassing capacitance up to the scan rate of  $500 \text{ mV s}^{-1}$  (Fig. 3c). In contrast, the capacitive performance of PICACTIF - a micro-meso high surface area carbon - was plotted in Fig. 3c, which was tested in our previous work [5]. Comparing with MCM20, PICACTIF with high SSA ( $2300 \text{ m}^2 \text{ g}^{-1}$  [5]) exhibits a rapid decay of capacitance with increasing scan rate, likely because of its lower mesoporous volume causing a lower efficient ionic mass-transfer of the embedded ionogel.

Equivalent series resistances of MCM20, MCM10 and MCM05 devices were measured at  $5$ ,  $9$  and  $7 \Omega \text{ cm}^2$  respectively from the Nyquist plots (Fig. 3d,e). These similar values are mainly derived from the ionogel bulk resistance and electrical resistance of the carbon electrodes, which are comparable to previous works [4,5]. The faster increase of the imaginary part of the impedance observed for the MCM20 sample evidences that the higher mesoporous volume of MCM20 facilitates the electrolyte accessibility in its larger pores [16]. As shown in Fig. 3f, the in-pore ionic resistance of MCM20 ( $14 \Omega \text{ cm}^2$ ) is only one-fifth of that of MCM10 ( $72 \Omega \text{ cm}^2$ ), further supporting the assumption that the mesopores favor for ion-transfer in solid ionogel electrolytes. Our mesoporous carbon monolith samples show promising performance in ionogel electrolytes for solid-state supercapacitor applications.

#### 4. Conclusions

Mesoporous carbon monoliths (MCM) were prepared using soluble salt as template. The pore sizes of MCM could be tuned from  $10$  to  $30 \text{ nm}$  by adjusting the ratio between salt and carbon sources. Thanks to high specific surface area and large porous volume, MCM exhibited attractive capacitive performance in EMITFSI. More specifically, the presence of large mesopores in MCM reduced the in-pore ionic resistance of electrolyte. As a result, binder-free MCM electrode could achieve a capacitance as high as  $75 \text{ F g}^{-1}$  ( $375 \text{ mF cm}^{-2}$ ) in ionogel electrolyte, showing great potential for all-solid-state supercapacitor applications.

#### Acknowledgements

PLT and PS thank the LABEX STORE-EX for support; SZ and NQZ thank the Natural Science Foundation of China (No. 51472177, 51771136) and China Scholarship Council.

#### References

- [1] P. Simon, Y. Gogotsi, Materials for electrochemical capacitors, *Nat. Mater.* 7 (2008) 845–854.
- [2] P. Simon, Y. Gogotsi, B. Dunn, Where do batteries end and supercapacitors begin? *Science* 343 (2014) 1210–1211.
- [3] J. Le Bideau, L. Viau, A. Vioux, Ionogels, ionic liquid based hybrid materials, *Chem. Soc. Rev.* 40 (2011) 907–925.
- [4] L. Nègre, B. Daffos, V. Turq, P.-L. Taberna, P. Simon, Ionogel-based solid-state supercapacitor operating over a wide range of temperature, *Electrochim. Acta* 206 (2016) 490–495.
- [5] L. Nègre, B. Daffos, P.-L. Taberna, P. Simon, Solvent-free electrolytes for electrical double layer capacitors, *J. Electrochem. Soc.* 162 (2015) A5037–A5040.
- [6] D.R. MacFarlane, N. Tachikawa, M. Forsyth, J.M. Pringle, P.C. Howlett, G.D. Elliott, J. Davis, M. Watanabe, P. Simon, C.A. Angell, Energy applications of ionic liquids, *Energy Environ. Sci.* 7 (2014) 232–250.
- [7] S. Wang, B. Hsia, C. Carraro, R. Maboudian, High-performance all solid-state micro-supercapacitor based on patterned photoresist-derived porous carbon electrodes and an ionogel electrolyte, *J. Mater. Chem. A* 2 (2014) 7997–8002.
- [8] Z. Chen, W. Ren, L. Gao, B. Liu, S. Pei, H.M. Cheng, Three-dimensional flexible and conductive interconnected graphene networks grown by chemical vapour deposition, *Nat. Mater.* 10 (2011) 424–428.

- [9] M.C. Liu, L.B. Kong, P. Zhang, Y.C. Luo, L. Kang, Porous wood carbon monolith for high-performance supercapacitors, *Electrochim. Acta* 60 (2012) 443–448.
- [10] H. Li, D. Yuan, C. Tang, S. Wang, J. Sun, Z. Li, T. Tang, F. Wang, H. Gong, C. He, Lignin-derived interconnected hierarchical porous carbon monolith with large areal/volumetric capacitances for supercapacitor, *Carbon* 100 (2016) 151–157.
- [11] S. Zhu, J.J. Li, C.N. He, N.Q. Zhao, E.Z. Liu, C.S. Shi, M. Zhang, Soluble salt self-assembly-assisted synthesis of three-dimensional hierarchical porous carbon networks for supercapacitors, *J. Mater. Chem. A* 3 (2015) 22266–22273.
- [12] S. Zhu, J.J. Li, L.Y. Ma, L.C. Guo, Q.Y. Li, C.N. He, E.Z. Liu, F. He, C.S. Shi, N.Q. Zhao, Three-dimensional network of N-doped carbon ultrathin nanosheets with closely packed mesopores: controllable synthesis and application in electrochemical energy storage, *ACS Appl. Mater. Interfaces* 8 (2016) 11720–11728.
- [13] P.-L. Taberna, P. Simon, J.F. Fauvarque, Electrochemical characteristics and impedance spectroscopy studies of carbon-carbon supercapacitors, *J. Electrochem. Soc.* 150 (2003) A292–A300.
- [14] C. Largeot, C. Portet, J. Chmiola, P.-L. Taberna, Y. Gogotsi, P. Simon, Relation between the ion size and pore size for an electric double-layer capacitor, *J. Am. Chem. Soc.* 130 (2008) 2730–2731.
- [15] R. Futamura, T. Iiyama, Y. Takasaki, Y. Gogotsi, M.J. Biggs, M. Salanne, J. Ségolini, P. Simon, K. Kaneko, Partial breaking of the Coulombic ordering of ionic liquids confined in carbon nanopores, *Nat. Mater.* 16 (2017) 1225–1232.
- [16] J. Gamby, P.-L. Taberna, P. Simon, J.F. Fauvarque, M. Chesneau, Studies and characterisations of various activated carbons used for carbon/carbon supercapacitors, *J. Power Sources* 101 (2001) 109–116.
- [17] Z. Lin, P.-L. Taberna, P. Simon, Graphene-based supercapacitors using eutectic ionic liquid mixture electrolyte, *Electrochim. Acta* 206 (2016) 446–451.